Nonlinear Microwave Optics in Liquid Suspensions of Shaped Microparticles

D. Rogovin, R. McGraw, W. Ho, R. Shih, H. R. Fetterman, and Bradley Bobbs

Abstract—**The unique properties of shaped microparticle suspensions make them suitable as candidate media for such active optical process as phase conjugate via degenerate four-wave mixing at microwave and millimeter wavelengths. We have generated up 250 mW of phase conjugate radiation, a medium composed of rod shaped carbon fibers suspended in a passive fluid dielectric that is maintained in a waveguide. The theory for the nonlinear optical properties of shaped particle suspensions is presented and shown to be in excellent agreement with the available experimental data.**

I. Introduction

UNTIL recently, attempts to achieve active phase control using nonlinear optical schemes have been limited to the visible and the infrared regions of the spectrum, employing laser beams as the driving fields [1]. Typical optical processes that are utilized include nonlinear phase shifting [2], optical phase conjugation [3], two beam coupling [4] and optical birefringence [5]. Efforts to extend these processes down to millimeter or microwave frequencies have, until recently [6]–[9], failed due to a lack of suitable nonlinear optical materials.

This lack of success in achieving nonlinear optical effects at microwave and millimeter wavelengths can be appreciated by considering the challenges one must overcome to achieve optical phase conjugation at these comparatively long wavelengths. In particular, contrast the four-wave mixing coefficient $\kappa = 16\pi^2\chi^{(3)}I_p/c\lambda$ at visible and microwave frequencies. Here I_p is the pump power, λ is the free space wavelength and $\chi^{(3)}$ is the third-order nonlinear susceptibility. At visible and infrared wavelengths, pump sources can readily achieve power levels of tens to hundreds of MW/cm^2. At cm wavelengths, standard laboratory power supplies are usually limited to under one kW/cm^2 as the beam cannot be focused down to spot sizes smaller than an optical wavelength due to diffraction effects. This five orders of magnitude reduction in pump power is further compounded by an additional four orders of magnitude decrease in κ, caused by the increase in λ that one encounters in going from the visible to the microwave region of the electromagnetic spectrum. Thus, κ scales as λ^{-3}. These considerations are summarized in Table I which reveals that active media with nonlinear susceptibilities on the order of 10^{-3} to 10^{-4} esu are required if one is to achieve optical phase conjugation at 18 GHz.

Artificial dielectrics, such as liquid suspensions of microparticles, are known to have exceptionally large nonlinear optical susceptibilities and might be suitable candidates as active media for microwave applications. Ashkin and Smith achieved self-focusing [10], optical bistability [11] and optical phase conjugation [12] with an aqueous suspension of 1000 Å polystyrene microspheres as the nonlinear medium and cw Argon-ion laser beams as the optical source. Third-order optical susceptibilities were found to be as large as 10^{-8} esu, five orders of magnitude greater than CS_2. Since the third-order susceptibility scales as the sixth power of the microparticle radius, it seems reasonable to consider scaling the particle size up to microns to realize nonlinear susceptibilities on the order of 10^{-2} esu, for microwave applications.

Unfortunately, this scheme is not viable since the mechanism responsible for the nonlinear optical properties for this class of media is too slow for the observation of any nonlinear effects at these wavelengths. More precisely, forces due to an electrostrictive interaction between the microparticle polarizability and the incident probe and pump beams give rise to microparticle density gratings which coherently scatter pump radiation to form a phase conjugate wave. The formation of these index gratings, essential for optical phase conjugation, requires that the microparticles translate a grating spacing, typically several optical wavelengths. At visible wavelengths, grating formation requires that the particles diffuse several microns through a viscous medium. If the host fluid is water, this requires several hundred milliseconds. Since the particle motion is essentially Brownian in nature, the response time scales inversely with the square of the grating spacing and directly with fluid viscosity. Scaling to millimeter or centimeter wavelengths increases the medium response time by six to eight orders of magnitude. This implies grating formation times that are on the order of days, not seconds which are not feasible as thermal currents will suppress the formation of these optical index gratings. Another complication arises from the fact that water is a strong absorber of microwave and millimeter wave radiation, so that a nonabsorbing host must be found. This requires a nonpolar fluid and care must be exercised to avoid coagulation of the microparticles.

Manuscript received July 22, 1991; revised February 25, 1992.

D. Rogovin, R. McGraw and W. Ho are with Rockwell Science Center, Thousand Oaks, CA 91360.

R. Shih and H. R. Fetterman are with the Department of Electrical Engineering, University of California, Los Angeles, Los Angeles, CA 90024.

B. Bobbs is with Rockwell International, Rocketdyne Division, Canoga Park, CA 91303.

IEEE Log Number 9201717.

TABLE I
DIFFICULTIES AT LONG WAVELENGTHS

Physical Parameter	Visible Wavelengths	Microwave/Millimeter Wavelengths
Wavelength	0.5 μ	1 cm–0.1 cm
Pump Intensity	10^8 W/cm^2	10^3 W/cm^2
Typical values of $\chi^{(3)}$	10^{-10} esu	10^{-10} esu
Optical Pathlength	2 mm	30 cm
κL	1.2	10^{-9}
Efficiency	gain	negligible

Another class of artifical dielectrics that can be potential active media at microwave and millimeter wavelengths are shaped microparticle suspensions [13]. This class of nonlinear materials have third-order optical susceptibilities that also scale as the square of the microparticle volume. Therefore they should have a sufficiently large nonlinear susceptibility to overcome the scaling characteristics of κ with radiation wavelength. In addition to the usual translational gratings (that are useless for our purposes), shaped particle suspensions also form orientational index gratings. These index gratings consist of periodic spatial arrangements in which the particles within a given region tend to be randomly oriented and regions in which some fraction of them are oriented in a direction specified by the polarization vector of the incident radiation. A major advantage of this class of index grating is that their formation requires only that the microparticles rotate into desired orientations; they do not have to translate. Thus, the response time is independent of grating spacing and therefore of wavelength. The grating formation time is on the order of the angle through which the particles rotate ($\Delta\Theta$), divided by the angular velocity, (Ω). Thus, the time scale involves the particle size ρ instead of the grating spacing Λ and the ratio of the orientational to the translational response times (τ_0/τ_T) is $(\rho/\Lambda)^2$. For 10 μ size particles, the orientational response time is seconds for typical nonpolar fluids. Although this is too long for some applications, it is sufficiently short that laboratory experiments can be conducted on a convenient timescale and the effects can be readily observed.

We have successfully carried out microwave phase conjugation [8] in shaped microparticle suspensions consisting of 0.01%–0.1% volume fractions of carbon fibers suspended in a 60% mineral oil-40% heptane host fluid mixture. Power levels of up to 250 mW, with only 14.65 W of pump power were generated at 18 GHz. The measured host fluid viscosity is 5 cp and the microparticle response time is on the order of ten seconds. The carbon fibers, which are ellipsoidal in shape with dimensions of 3 μm × 3 μm × 8 μm, act as perfect conductors at 18 GHz. The host fluid is highly transparent to microwave radiation and at 18 GHz the suspension's absorption constant is 140 cm^{-1}. The small size of the particles relative to the radiation wavelength ensures that scattering loss's are negligible. The suspension is maintained in a metal waveguide, with dimensions of 1.46 cm × 1.46 cm × 72 cm. The waveguide acts to enhance the microwave intensity and also reduces thermal eddy currents thus allowing the formation of microparticle orientational index gratings.

This paper is divided into four parts of which this, the Introduction, is the first. Section II outlines the theoretical model used to describe the interaction of shaped microparticles with coherent radiation. In Section III, we present our findings regarding microwave phase conjugation in liquid suspensions of shaped microparticles. Finally, in Section IV we summarize our studies and present our conclusions regarding nonlinear optics at these long wavelengths.

II. PHYSICS OF SHAPED MICROPARTICLE SUSPENSIONS

We assume a monodisperse suspension of shaped microparticles whose polarizability tensor $\alpha(\theta, \phi)$ is

$$\alpha(\theta, \phi) = \alpha_S \boldsymbol{I} + \tfrac{1}{3}\beta \boldsymbol{K}(\theta, \phi). \tag{2.1}$$

Here (θ, ϕ) specifies the orientation of the microparticle polarizability relative to a lab fixed reference frame, α_S is the isotropic component of the polarizability, β is the anisotropic component, $\boldsymbol{I}$ is the unit tensor and $\boldsymbol{K}(\theta, \phi)$ is the orientation tensor whose components are

$$\boldsymbol{K}(\theta, \phi) = \begin{matrix} 3\sin^2\theta\cos^2\phi - 1 & 3\sin^2\theta\sin\phi\cos\phi & 3\sin\theta\cos\theta\sin\phi \\ 3\sin^2\theta\sin\phi\cos\phi & 3\sin^2\theta\sin^2\phi - 1 & 3\sin\theta\cos\theta\cos\phi \\ 3\sin\theta\cos\theta\sin\phi & 3\sin\theta\cos\theta\cos\phi & 3\cos^2\theta - 1. \end{matrix} \tag{2.2}$$

If the microparticles are illuminated by an electromagnetic field [denoted by $\boldsymbol{E}(\boldsymbol{r}, t)$], they each acquires an induced dipole moment $\boldsymbol{p}(\theta, \phi; \boldsymbol{r}, t) = [\alpha_S \boldsymbol{I} + (1/3)\beta \boldsymbol{K}(\theta, \phi)] \cdot \boldsymbol{E}(\boldsymbol{r}, t)$. This induced dipole moment couples back to the electromagnetic field giving rise to an interaction potential $U(\theta, \phi; \boldsymbol{r}, t)$, equal to

$$U(\theta, \phi; \boldsymbol{r}, t) = -\tfrac{1}{2}\overline{\boldsymbol{p}(\theta, \phi; \boldsymbol{r}, t) \cdot \boldsymbol{E}(\boldsymbol{r}, t)}. \tag{2.3}$$

The overbars imply a time average that is long compared to the optical period, but short compared to the medium response time. The interaction potential gives rise to an electrostrictive force $\boldsymbol{F}(\boldsymbol{r}, t) = -\nabla U(\theta, \phi; \boldsymbol{r}, t)$ that tends to move the particles towards regions where $U(\theta, \phi; \boldsymbol{r}, t)$ is a minimum. This force favors particular particle orientations and weakly couples the center-of-mass and orientational coordinates. $U(\theta, \phi; \boldsymbol{r}, t)$ also generates a torque $\Gamma(\theta, \phi; \boldsymbol{r}, t) = -\boldsymbol{L}U(\theta, \phi; \boldsymbol{r}, t)$ where $\boldsymbol{L}$ is the particle angular momentum operator. This field-induced torque tends to rotate the particles in a direction specified by the vector polarization of the radiation field. When the suspension is irradiated by a plane polarized beam, the particles tend to point in a given direction and the propaga-

tion features of incident radiation will depend upon beam polarization, giving rise to optical birefringence [6], [7]. If the suspension is irradiated by more than one field, then coherent interference between the electromagnetic waves will give rise to a modulation of the preferred particle orientation. This modulation of the dielectric constant is an optical index grating that can be utilized for phase conjugation.

If the interaction potential is time dependent, as occurs with a single beam or degenerate beams, then in steady-state the particle orientational distribution $n(\theta, \phi; \boldsymbol{r}) = n_0 \exp[-U(\theta, \phi; \boldsymbol{r})/\mathrm{kT}]/Z$ with n_0 the particle density in the absence of external fields and Z the partition function.

We first consider the case of a single microwave or millimeter wave pump beam irradiating a shaped microparticle suspension that is kept in a waveguide. The incident pump beam is written as $\boldsymbol{E}(\boldsymbol{r}, t) = \boldsymbol{e}A(\boldsymbol{r}) \cos[\boldsymbol{K} \cdot \boldsymbol{r} - \omega t]$ where $\boldsymbol{e}$ is the unit polarization vector, $A(\boldsymbol{r})$ is the field amplitude, $\boldsymbol{K}$ the propagation wavevector and ω is the frequency. The interaction potential is

$$U(\theta, \phi; \boldsymbol{r}, t) = -\tfrac{1}{2}A(\boldsymbol{r})^2[\alpha_S + \tfrac{1}{3}\beta \boldsymbol{e} \cdot \boldsymbol{K}(\theta, \phi) \cdot \boldsymbol{e}^*]. \tag{2.4}$$

If the pump beam intensity is unaffected by the medium, the microparticle orientational distribution for a suspension irradiated plane electromagnetic wave is

$$n(\theta, \phi; \boldsymbol{r}) = n_0 \exp[\tfrac{1}{3}g_1 \boldsymbol{e} \cdot \boldsymbol{K}(\theta, \phi) \cdot \boldsymbol{e}^*] \Big/ \int d\phi \int d\theta \sin\theta \exp[g_1 \boldsymbol{e} \cdot \boldsymbol{K}(\theta, \phi) \cdot \boldsymbol{e}^*] \tag{2.5}$$

where $g_1 = \beta A^2/4\ \mathrm{kT}$ is a dimensionless field strength. The isotropic part of the microparticle polarizability is coupled to the particle's translational degrees of freedom and does not enter into the problem. For the shaped microparticle distribution used in our microwave experiments, $\beta = 10^{-11}$ esu, and for a pump intensity of 20 W/cm^2, $g_1 = 5$. In the weak field limit, where $g_1 \ll 1$, only a small fraction, $\delta n(\theta, \phi)$ of the microparticles are oriented by the pump beam

$$\delta n(\theta, \phi) = n_0 g_1 \boldsymbol{e} \cdot \boldsymbol{K}(\theta, \phi) \cdot \boldsymbol{e}^*. \tag{2.6}$$

In the strong field regime, where $g \gg 1$, most of the microparticles are aligned by the pump beam. If the pump wave is linearly polarized, then the microparticle orientational distribution is

$$n_z(\theta, \phi) = (g_1/\pi)^{1/2} n_0 \exp[g_1 \cos^2\theta]/\mathrm{erf}[g_1^{-1/2}]. \tag{2.7}$$

The macroscopic dipole moment $\boldsymbol{P}(\boldsymbol{r}, t) \equiv \langle \boldsymbol{p}(\theta, \phi; \boldsymbol{r}, t) n(\theta, \phi; \boldsymbol{r}, t) \rangle$ where the brackets imply an angular average over (θ, ϕ). If U is independent of position, the particle density will be spatially uniform and

$$\boldsymbol{P}(\boldsymbol{r}, t) = \alpha_S n_0 \boldsymbol{E}(\boldsymbol{r}, t) + \tfrac{1}{3}\beta \langle n(\theta, \phi; t) \boldsymbol{K}(\theta, \phi) \rangle \cdot \boldsymbol{E}(\boldsymbol{r}, t). \tag{2.8}$$

The first term on the rhs of (2.8) is negligible. The next term depends critically on the anisotropic properties of the suspension; it vanishes if $n(\theta, \phi; t) = n_0$. In the limit that $U/\mathrm{kT} \ll 1$, this term can be written as

$$\delta \boldsymbol{P}(\boldsymbol{r}, t) = n_0 g_1 \langle \boldsymbol{e} \cdot \boldsymbol{K}(\theta, \phi) \cdot \boldsymbol{e}^* \boldsymbol{K}(\theta, \phi) \rangle \cdot \boldsymbol{E}(\boldsymbol{r}, t). \tag{2.9}$$

If we define $Q_{ij,kl} = \langle K_{ij}(\theta, \phi) K_{kl}(\theta, \phi) \rangle$, then it is obvious that only those components of $\delta \boldsymbol{P}(\boldsymbol{r}, t)$ are nonzero for which all of the indices are the same or ones in which pairs are equal. Thus, if all of the beams are linearly polarized in the same direction (taken to define the z-direction), then only the z-component of $\delta \boldsymbol{P}(\boldsymbol{r}, t)$ is nonzero.

The microparticle suspensions dynamics are described by the Planck-Nernst (PN) equation [13] for the particle density, $n(\theta, \phi; \boldsymbol{r}, t)$. This equation specifies how $n(\theta, \phi; \boldsymbol{r}, t)$ changes in time under the action of field-induced forces, torques and diffusion due to Brownian motion. At microwave and millimeter wavelengths, only the orientational coordinates vary on the time scales of interest and we can ignore changes in the microparticle density at a given point $\boldsymbol{r}$.

The PN equation is basically a conservation equation in the sense that the change in density of particles pointing in a given direction (θ, ϕ) obeys $\partial n(\theta, \phi)/\partial t = -\boldsymbol{L} \cdot \boldsymbol{J}(\theta, \phi)$, with $\boldsymbol{J}(\theta, \phi)$ the particle flux. There are two contributions to $\boldsymbol{J}$: a diffusive current $\boldsymbol{J}_D(\theta, \phi) = -\Theta_0 \boldsymbol{L} n(\theta, \phi)$ and a drift current $\boldsymbol{J}_F(\theta, \phi) = \Theta_0[\Gamma(\theta, \phi)/\mathrm{kT}] n(\theta, \phi)$. The PN equation is then

$$\partial n(\theta, \phi)/\partial t + \Theta_0 \boldsymbol{L}^2 n(\theta, \phi) = -\Theta_0/kT \boldsymbol{L} \cdot [\Gamma(\theta, \phi) n(\theta, \phi)]. \tag{2.10}$$

In steady-state, $\partial n(\theta, \phi)/\partial t = 0$ and the solution of (2.10) is the Maxwell–Boltzman distribution. In the weak field regime, where $U/\mathrm{kT} \ll 1$, only a small fraction of the microparticles $\delta n \ll n_0$ are influenced by the applied fields and the PN equation can be solved perturbatively. Setting $n(\theta, \phi) = n_0 + \delta n(\theta, \phi)$ where $\delta n(\theta, \phi)$ is of order U/kT, we have

$$\partial \delta n(t; \theta, \phi)/\partial t + \Theta_0 \boldsymbol{L}^2\, \delta n(t; \theta, \phi) = (\Theta_0/kT) n_0 L^2[U(t; \theta, \phi)]. \tag{2.11}$$

The angular dependence of $U(\theta, \phi)$ is given by the matrix elements of $\boldsymbol{K}(\theta, \phi)$. Since these elements can all be expressed as a linear combination of the $Y_2^m(\theta, \phi)$ it follows that $\boldsymbol{L}^2[U(\theta, \phi)] = 6U(\theta, \phi)$. The orientational diffusion time is defined by, $\tau_R = 1/6\Theta_0$, and noting that $\delta n(t; \theta, \phi) = 0$ at $t = 0$,

$$\delta n(t, \theta, \phi) = n_0 \int_0^t dt' \exp\left[-\frac{(t - t')}{\tau_R}\right] \frac{U(t', \theta, \phi)}{kT}. \tag{2.12}$$

In the strong field regime, where $U/\mathrm{kT} \geq 1$, most of the microparticles are oriented by the applied fields. In

that case (2.15d) must be solved exactly. This can be done by expanding the density in the spherical harmonics

$$n(t;\theta,\phi) = \sum_{l=0}^{l=\infty} c_{2l}(t)\, Y_{2l}^{0}(\theta,\phi) \tag{2.13}$$

where we have used the fact that symmetry requires that only the even-order terms contribute to the sum. The resultant equations are of the form $dn(t)/dt = An(t)$ where A is a non-Hermitean matrix and can be solved numerically.

III. Microwave Phase Conjugation

The theory for microwave phase conjugation using a shaped particle suspension is discussed in III-A. In III-B and III-C the detailed properties of the suspension and our experimental procedure are reviewed. In III-D the experimental observations are presented and correlated them with theory.

A. Theoretical Formulation

In our phase conjugation experiments, the suspension was irradiated by two, degenerate microwave beams that wrote a volume index grating. The vector sum of these two write beams, each oscillating at the frequency ω, is denoted by $\boldsymbol{E}_D(\boldsymbol{r}, t) = \boldsymbol{E}_1(\boldsymbol{r}, t) + \boldsymbol{E}_2(\boldsymbol{r}, t)$, where

$$\boldsymbol{E}_j(\boldsymbol{r}, t) = \tfrac{1}{2}E_{0j}[A_j(z, t)\boldsymbol{e}_x + B_j(z, t)\boldsymbol{e}_y] \cdot \exp[i(\boldsymbol{K}_j \cdot \boldsymbol{r} - \omega t)] + cc \tag{3.1}$$

with E_{0j} and $\boldsymbol{K}_j$ the initial amplitude and wave vector of the jth beam. The functions $A_j(z, t)$, $B_j(z, t)$ specify the two polarization components of the jth beam as it propagates through the shaped microparticle suspension, and $\boldsymbol{e}_x$ ($\boldsymbol{e}_y$) is a unit vector in the x (y) direction. The interaction potential, $U_D(\boldsymbol{r}, \Omega)$ between the particles and the write beams is

$$U_D(\boldsymbol{r}) = g[A_1A_2^*K_{xx} + B_1B_2^*K_{xx} + (A_1B_2^* + B_1A_2^*)K_{xy}] \cdot \exp[i\boldsymbol{Q} \cdot \boldsymbol{r}] + cc \tag{3.2}$$

with $\boldsymbol{Q} \equiv \boldsymbol{K}_1 - \boldsymbol{K}_2$, $g \equiv \beta E_{01}E_{02}/4\ \mathrm{kT}$ and $K_{jk} \equiv \boldsymbol{e}_j \cdot \boldsymbol{K} \cdot \boldsymbol{e}_k$. For static index gratings, the portion of the microparticle distribution function of interest is $\delta n(t;\theta,\phi) = -n_0U_D(\boldsymbol{r},\theta,\phi)/\mathrm{kT}$. The $\mu\nu$ component of the optical index tensor grating, $\delta\epsilon_{\mu\nu}(\boldsymbol{r},\theta,\phi)$ arising from these microparticle gratings, is given by

$$\delta\epsilon_{\mu\nu}(\boldsymbol{r}) = -\tfrac{1}{3}n_0g\langle[A_1A_2^*K_{xx} + B_1B_2^*K_{xx} + (A_1B_2^* + B_1A_2^*)K_{xy}]\alpha_{\mu\nu}\rangle \cdot \exp[i\boldsymbol{Q} \cdot \boldsymbol{r}] + cc \tag{3.3}$$

The microparticle distribution is, to first-order in the write beams,

$$n(\boldsymbol{r}) = n_0 - \tfrac{1}{3}n_0g[A_1A_2^*K_{xx} + B_1B_2^*K_{xx} + (A_1B_2^* + B_1A_2^*)K_{xy}]\exp[i\boldsymbol{Q} \cdot \boldsymbol{r}] + cc \tag{3.4}$$

The terms that are proportional to g give rise to the orientational grating and tend to point in a direction specified by the write beams.

In standard optical phase conjugation all of the beams are focussed into the medium at the same time; and energy can be exchanged between the probe and conjugate waves. Furthermore there are two gratings that are formed by the pump and probe beams. These gratings have spatial periodicities of $\boldsymbol{K} \pm \boldsymbol{Q}$. Each grating will diffract the counterpropagating pump and form a conjugate beam.

For the case of collinear pump and probe beams, as was used in the waveguide experiments, there are significant difficulties associated with beam discrimination. To this end, we modulated one of the pump beams so as to ensure identification of conjugate beam photons. When this beam coherently diffracted off of the grating formed by the unmodulated pump and probe waves, the conjugate beam so formed maintained the original amplitude modulation. On the other hand, the grating formed by the modulated pump and probe wave will also be static because the medium cannot respond to a signal that changes at 300 Hz. However, since the beam is amplitude and not phase modulated, the time averaged response of the medium will not be zero, but rather one-half that for an unmodulated beam. The counterpropagating pump beam will scatter off of this static grating to form an unmodulated phase conjugate wave. This beam is unmodulated and cannot be distinguished from back reflections of the probe beam. Although we can model the experiment outlined in Section III-C by including only the orientational grating set up by the unmodulated pump and probe beams, it is of interest to examine the effects of both gratings.

The nonlinear polarization vector is

$$\boldsymbol{P}(\boldsymbol{r}, t) = n_0\frac{\beta^2}{18\ \mathrm{kT}}\langle[\overline{\boldsymbol{E}\cdot\boldsymbol{K}\cdot\boldsymbol{E}}]\boldsymbol{K}\cdot\boldsymbol{E}(\boldsymbol{r}, t)\rangle \equiv \Delta\epsilon\cdot\boldsymbol{E} \tag{3.5}$$

where we have used the fact that an average of $\langle\boldsymbol{K}(\theta,\phi)\rangle = 0$ for an isotropic distribution. For phase conjugation,

$$\boldsymbol{E}(\boldsymbol{r}, t) = \sum_{j=1,2,p,c} E_{0j}(\boldsymbol{r}, t)\boldsymbol{e}_j \exp[i(\omega_j t - \boldsymbol{k}_j \cdot \boldsymbol{r})] + cc \tag{3.6}$$

where $j = 1(2)$ is the modulated (unmodulated) pump beam, $j = p$ the probe wave, and $j = c$ the phase conjugate beam. Here $E_{0j}(\boldsymbol{r}, t)$ is the complex field amplitude, $\boldsymbol{e}_j$ the normalized polarization vector and $\omega_j(\boldsymbol{k}_j)$ the frequency (wave vector) of the jth beam. Only the amplitude modulated pump beam and the phase conjuage wave are time-dependent. In the fully degenerate case: $\omega_j = \omega$, $\boldsymbol{k}_1 = -\boldsymbol{k}_2 = \boldsymbol{K}$ and $\boldsymbol{k}_p = -\boldsymbol{k}_c = \boldsymbol{Q}$. Since the probe and conjugate waves vary as $\exp[i(\omega t \pm \boldsymbol{Q} \cdot \boldsymbol{r})]$, it follows that only those terms with the same phasors will contribute to the form the conjugate wave. The component the third-order polarization of interest, $\boldsymbol{P}_{\mathrm{NL}}(\boldsymbol{r}, t) = \boldsymbol{P}_{\mathrm{NL}}^{a+} + \boldsymbol{P}_{\mathrm{NL}}^{a-}$, with $\boldsymbol{P}_{\mathrm{NL}}^{a+}$ ($\boldsymbol{P}_{\mathrm{NL}}^{a-}$) is the nonlinear polarizability associated with the conjugate wave (amplification of the probe

beam):

$$\boldsymbol{P}_{\mathrm{NL}}^{a,+}(\boldsymbol{r}, t) = n_0 \beta g E_p^* [\tfrac{1}{2} \langle (\boldsymbol{e}_p^* \cdot \boldsymbol{K} \cdot \boldsymbol{e}_1) \boldsymbol{K} \cdot \boldsymbol{e}_2 \rangle + \langle (\boldsymbol{e}_p^* \cdot \boldsymbol{K} \cdot \boldsymbol{e}_2) \boldsymbol{K} \cdot \boldsymbol{e}_1 \rangle f(t)] \cdot \exp[i(\omega t + \boldsymbol{Q} \cdot \boldsymbol{r})] + cc. \quad (3.7)$$

A similar expression holds for $\boldsymbol{P}_{\mathrm{NL}}^{a-}$. The factor of $1/2$ arises from the averaging of the grating created by the amplitude modulated pump beam and the probe wave. The quantity $f(t)$ is the amplitude modulation function.

Next, we construct the wave equations for the propagation of the phase conjugate beam and the probe wave for steady-state situations. Inserting the nonlinear polarization into the wave equation, separating the modulated and unmodulated terms probe and conjugate waves

$$(2\boldsymbol{Q} \cdot \nabla + Q/2L_S) E_C^{\mathrm{mod}} \boldsymbol{e}_C = \mathrm{in}_0 \beta Q^2 (g/9) \langle (\boldsymbol{e}_P \cdot \boldsymbol{K} \cdot \boldsymbol{e}_2) \boldsymbol{e}_1 \cdot \boldsymbol{K} \rangle E_P^* \quad (3.8a)$$

$$(2\boldsymbol{Q} \cdot \nabla + Q/2L_S) E_C^{\mathrm{mod}} \boldsymbol{e}_C = +\tfrac{1}{2} \mathrm{in}_0 \beta Q^2 (g/9) \langle (\boldsymbol{e}_P \cdot \boldsymbol{K} \cdot \boldsymbol{e}_1) \boldsymbol{e}_2 \cdot \boldsymbol{K} \rangle E_P^{un*} \quad (3.8b)$$

$$(2\boldsymbol{Q} \cdot \nabla - Q/2L_S) E_p^{\mathrm{mod}} \boldsymbol{e}_p = -\mathrm{in}_0 \beta Q^2 (g/9) \langle (\boldsymbol{e}_C^* \cdot \boldsymbol{K} \cdot \boldsymbol{e}_2) \boldsymbol{e}_1 \cdot \boldsymbol{K} \rangle E_C^* \quad (3.8c)$$

$$(2i\boldsymbol{Q} \cdot \nabla - Q/2L_S) E_p^{un} \boldsymbol{e}_p = \tfrac{1}{2} \mathrm{in}_0 \beta Q^2 (g/9) \langle (\boldsymbol{e}_C^* \cdot \boldsymbol{K} \cdot \boldsymbol{e}_1) \boldsymbol{e}_2 \cdot \boldsymbol{K} \rangle E_C^{\mathrm{mod}*}. \quad (3.8d)$$

The angular brackets imply an orientational average over an isotropic distribution. Note that the total conjugate and probe beams enter into the nonlinear polarization for the modulated components. This feature arises because for amplitude modulated functions, $f(t) = f(t)^2$. Also only the unmodulated components enter into the nonlinear polarizations for $\epsilon_C^{\mathrm{unmod}}$ and $\epsilon_p^{\mathrm{unmod}}$. In the small signal regime energy transfer between the probe and conjugate beams is negligible and we can replace ϵ_p^* in (3.8a) and (3.8b) by the initial probe beam and integrate these equations directly. This gives

$$\epsilon_C^{\mathrm{mod}} = \mathrm{in}_0 QLg\beta/9 \langle (\boldsymbol{e}_P \cdot \boldsymbol{K} \cdot \boldsymbol{e}_2) \boldsymbol{e}_1 \cdot \boldsymbol{K} \cdot \boldsymbol{e}_C \rangle E_P^*(0) \equiv i\kappa L E_P^*(0) \quad (3.9a)$$

$$\epsilon_C^{un} = \mathrm{in}_0 QLg\beta/18 \langle (\boldsymbol{e}_P \cdot \boldsymbol{K} \cdot \boldsymbol{e}_2) \boldsymbol{e}_1 \cdot \boldsymbol{K} \cdot \boldsymbol{e}_C \rangle E_P^*(0) \equiv \tfrac{1}{2} i\kappa L E_P^*(0). \quad (3.9b)$$

The depth of the grating formed by the modulated pump and probe beams is one-half that of the grating formed by the modulated pump and probe beams. In the small signal regime, the intensity of the modulated conjugate wave is $(\kappa L)^2 I_P$ while that of the unmodulated beam is $(1/4)(\kappa L)^2 I_P$, provided the pump beams are parallel polarized as was done in the experiment.

For the case in which the probe beam is polarized orthogonal to the two pump waves $\kappa L = (8\pi/15) n_0 \beta g L/\lambda$. For typical suspensions, $n_0 \approx 10^8\ \mathrm{cm}^{-3}$, $\beta \approx 10^{-11}\ \mathrm{cm}^3$, $L/\lambda \approx 100$ and $g \approx 1$. Thus, κL is on the order of 0.2; implying efficiencies on the order of a few percent at cm wavelengths.

B. Nonlinear Medium

Various types of shaped microparticle suspensions were investigated, including aluminum platelets (used in metallic paints), chromium dioxide microrods (used in magnetic recording media), ground up alumina fibers, silicon carbide fibers, boron fibers, zinc sulfide, guanine platelets (used in rheoscopic fluids (Kalliroscope Corp., Groton, MA)), liquid crystals, ferrofluids, iron fillings, and even magnetic bacteria! Severe problems exist with those materials such as microwave and millimeter wave attenuation, particle agglomeration, unstable particle suspension, irregular eddy currents created by nonuniform thermal effect, and insufficient orientational susceptibility difference. The medium finally found to exhibit a significant and controllable Kerr effect was a suspension of short graphite fibers 7 to 8 microns in diameter. These fibers are available commercially (''Fortifil 5'' from Great Lakes Carbon) in 3 mm lengths, and ground up to yield lengths primarily in the range from 30 to 40 microns. Their low density helps to keep them in suspensions. The conductivity of graphite is sufficiently high on the order of 10^5 mho/m. The high conductivity of graphite is crucial in dispersing the particles in suspension. Dielectric particles tend to clump together due to the surface charges accumulated by the particles. Since one requirement of the suspending fluid is to be nonpolar due to the fact that polar solutions absorb microwave and millimeter wave radiation, the surface charges cannot dissipate. Therefore, the advantage of highly conductive microparticles is that they do not have local charge imbalance that would cause them to clump.

The suspending fluid used in the present study consists of a binary mixture of 60% mineral oil and 40% heptane. A maximum suspension stability of around 30 minutes was obtained which is adequate to perform the experiment. The resulting suspension with graphite particles with 0.1 volume percent is highly transparent, having loss lengths (1/e attenuation) of 140 cm at 18 GHz and 54 cm at 94 GHz. It is not known what fraction of the loss is due to scattering, although a small fraction is expected since the particles are much smaller than the wavelength.

C. Experimental Formulation

The experiments were conducted in a single-mode hollow metal waveguide to minimize thermal convection currents which might disrupt reorientation of the particles, to maximize signal intensity, and to allow interaction lengths limited only by absorption. These advantages are offset

by the difficulties encountered in discriminating between the various collinear waves emanating from the medium. The anisotropic characteristics of elongated microparticle suspensions give rise to a polarization dependence in $\chi^{(3)}$ which allows the use of the geometry utilized for isolating the conjugate wave depicted in Fig. 1. The polarizations of the probe and conjugate waves are linear and parallel to each other, but orthogonal to both the pump waves. Pump wave #1 is amplitude modulated at 300 Hz, while pump wave #2 and the probe are unmodulated. Two anisotropic volume gratings are created by the probe wave interacting with each of the pumps. Although one of the pump waves is amplitude modulated, neither grating is modulated because the medium response time (≈ 10 s) is much slower than the modulation period. Consequently, only the grating which scatters pumps wave #1 will generate phase conjugate radiation which is amplitude modulated at 300 Hz. This radiation is easily distinguished from the unmodulated probe reflection off the interfaces at the ends of the sample chamber. Scattering of pump #2 will produce an unmodulated phase conjugate wave which, however, cannot be readily distinguished from the reflected probe. The polarization of each pump wave is rotated by 90° as it scatters to form a conjugate wave. As shown schematically in Fig. 1, an rf oscillator at a frequency tunable around 18 GHz drives a traveling wave tube (TWT) amplifier which produces a maximum continuous power of 20 W. A 3-dB directional coupler splits the power equally to form the counterpropagating pump wave #2 and the probe wave. The probe wave goes through a variable attenuator and feeds into the H-plane port of the orthogonal-mode transducer (OMT) #1. An OMT is a waveguide analog of an optical polarizing beamsplitter which enables us to separate and combine beam polarizations. The probe wave passes through the 72-cm sample chamber inside a square waveguide of 1.36-c,2 cross sectional area and terminates at the H-plane port of OMT #2. The liquid sample is contained by two TFE windows. Pump wave #1 is created by taking a fraction of the rf power via a 6-dB coaxial coupler. It is then square-wave modulated by a p-i-n diode at 300 Hz and amplified by a lower power amplifier with a maximum output of 100 mW. This modulated pump wave is fed into the E plane port of OMT #1. The modulated conjugate beam exits the H plane port of OMT #1 and is detected by a lock-in amplifier via the 10 dB directional coupler. The leakage from the E-plane to the H-plane port of OMT #2 is about −40 dB, so the power reaching the detector from pump wave #2 is below the detection limit.

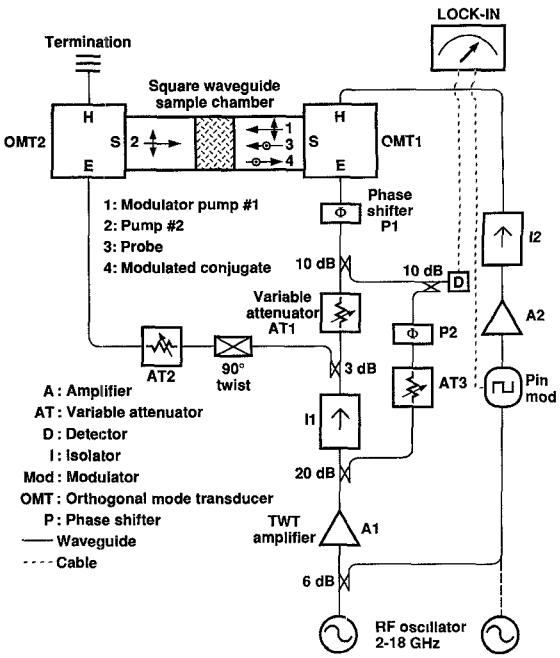

Fig. 1. Experimental configuration for demonstrating phase conjugation in a waveguide at 94 GHz.

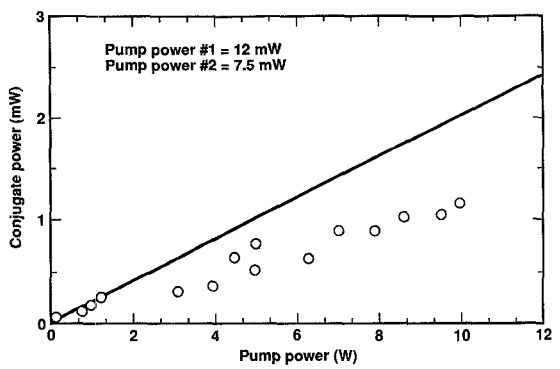

Fig. 2. Depicts the phase-conjugate power as a function of the probe power for the case in which the power of the modulated pump #1 is 12 mW and the cw pump #2 is 7.5 W.

D. Experimental Results and Comparison with Theory

Fig. 2 depicts the phase-conjugate power as a function of the probe power for the case in which the power of the modulated pump #1 is 12 mW and the cw pump #2 is 7.5 W. The phase-conjugate power varies linearly with probe power as expected and is 1 mW at a probe power of 10 W, corresponding to a nonlinear reflectivity of approximately 0.01%. If we employ the values of β and n_o obtained from the optical-birefringence measurements, we obtain a theoretical average value of 0.02%. The discrepancy can be attributed partially to slight differences between the two suspensions and is discussed below. The low reflectivity can be attributed partially to the unconventional power ratios used in the present experiment in which the modulated pump has much less power than the probe wave.

The efficiency of the phase conjugate wave can be increased significantly if the power of the first pump is as great as that of the second pump, and the probe power reduced accordingly. It is implemented by replacing the low power amplifier A2 by a 10 W cw TWT amplifier in Fig. 1. The probe power can be decreased by the setting of the attenuator #1. Fig. 3 depicts the phase-conjugate power as a function of the probe power for the case in which the power of the modulated pump #1 is 8 W and cw pump #2 is 7.5 W. The phase conjugate power varies

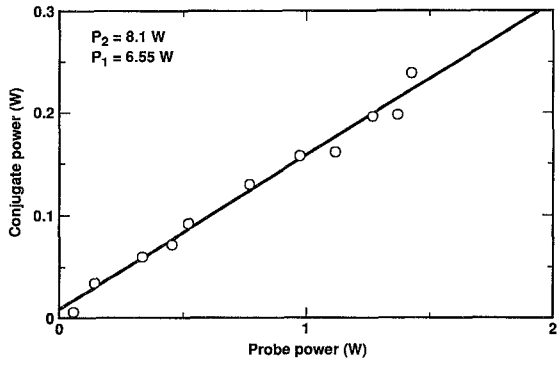

Fig. 3. Depicts the phase-conjugate power as a function of the probe power for the case in which the power of the modulated pump #1 is 8 W and cw pump #2 is 7.5 W.

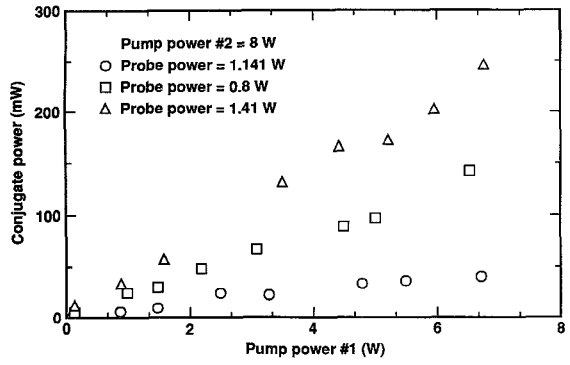

Fig. 4. Depicts the phase-conjugate power as a function of the power of the unmodulated pump beam for the cases in which the probe power is 0.141 W, 0.8 W and 1.41 W.

linearly with the probe power as expected and corresponding to a nonlinear high efficiency of approximately 15%.

Measurements were also performed by keeping the probe power constant and varying the power of pump #1. Pump #2 was kept constant at 8 W. The measurements were done with three constant probe powers of 0.141 W, 0.8 W, and 1.41 W. In all case, the conjugate power varies linearly with pump power #1 which indicate that the measurements are still within the small signal regime. These measurements are presented in Fig. 4.

The transient evolution of the conjugate power is depicted in Fig. 5. It is obtained by first having the steady probe and modulated pump #1 initially on and then switching on pump #2, at $t = 0$. As soon as the second pump wave is switched on, a grating begins to form that diffracts pump #1 to produce a modulated conjugate wave which is observed on the lock in amplifier. Thus the transient behavior of the modulated conjugate wave reflects the formation and approach to steady state of the orientational grating formed by the nonlinear interaction of the probe and pump #2 waves. Pump wave #2 is subsequently turned off at time $t = 22$ seconds to allow the index grating to deteriorate due to thermal diffusion, leading to the observed decay of the modulated phase conjugate signal. The medium has grating formation and decay times of approximately 10 seconds, which is a factor of three faster than the earlier Mach–Zehnder interferometer experiment as well as the theoretical prediction of 33 seconds. This discrepancy implies that the particle size is somewhat smaller for this suspension than the one employed in the birefringence experiments and is consistent with the smaller than expected reflectivity measurement.

Confinement inside a single mode waveguide prevents the propagation of wavefront perturbations in this experiment. Phase conjugation therefore reduces to one dimension, capable only of correcting for longitudinal phase error. A phase shifter can be used to induce this phase error by inserting it in the probe's path before the H-plane port of OMT #1, as shown in Fig. 1. The phase information of the conjugate signal can be obtained by comparing it with a reference which is taken from the TWT amplifier via a 20-dB directional coupler. Variable attenuator #3

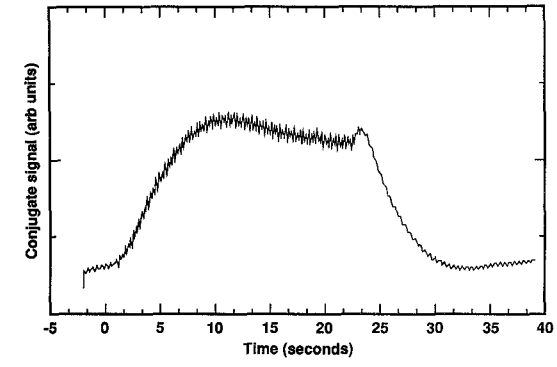

Fig. 5. The transient evolution of the conjugate power.

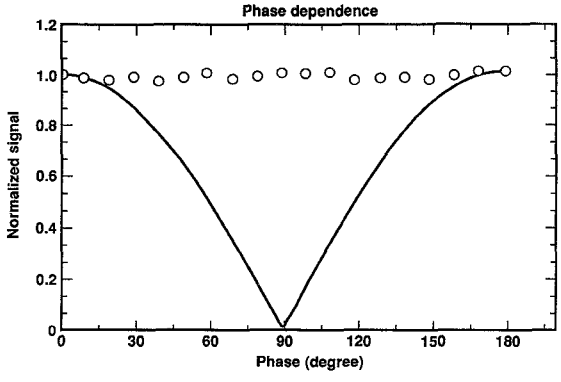

Fig. 6. Shows the equilibrium conjugated signal power (circles) as a function of the settings of phase shifter #1. For comparison, the solid curve represents the signal which is not conjugated.

and phase shifter #2 are inserted for proper adjustment of the reference which is combined with the conjugate beam via a 10 dB directional coupler. Phase shifter #2 is adjusted so that a maximum signal is shown on the lock-in amplifier. As phase shifter #1 is varied, the signal at the lock-in amplifier should not vary if the phase is truly corrected by the phase-conjugation process. In these measurements, the actual dynamics of the phase correction process is observed due to the slow response of the medium (time constant $\approx$ 10 s). The signal first decreases and then returns to its initial value as phase shifter #1 is varied. Fig. 6 shows the equilibrium conjugated signal power (circles) as a function of the settings of phase shif-

ter #1. For comparison, the solid curve represents the signal which is not conjugated. The same experiment was conducted on the secondary peak at 50 MHz, and phase conjugation was again observed.

IV. Discussion and Conclusions

Until now nonlinear optics has focused on visible and infrared wavelengths. This is due to the lack of suitable materials that can be used as the active medium in the microwave/millimeter wave region of the spectrum. In particular, since $\kappa \propto \lambda^{-3}$, there is a nine orders of magnitude decrease in κ, due to the increase in λ that one encounters in going from the visible to the microwave region of the spectrum. These considerations suggest that phase conjugation cannot be achieved at long wavelengths, unless novel materials can be found to overcome these difficulties.

Our studies indicate that shaped particle suspensions are well suited for achieving certain classes of nonlinear optical phenomena at microwave and millimeter wavelengths. Specifically, since they are highly polarizable their third-order susceptibilities are very large, approximately nine orders of magnitude greater than CS_2. Thus, low microwave power sources will generate large changes in the dielectric constant of the suspension. This feature of suspension electrodynamics can be readily exploited for such static third-order processes as optical birefringence and phase conjugation via degenerate four-wave mixing. Furthermore, the mechanism by which these changes in the suspension's dielectric constant are achieved involves rotation of the microparticles in a direction specified by the applied fields. Thus in the diffusive regime, the response time depends only the particle size and shape, the fluid viscosity and temperature of the host.

Crucial to long wavelength applications is the fact that the response time for orientational gratings in shaped microparticle suspensions is independent of radiation wavelength or grating spacing. This feature can be appreciated by noting that for translational or density gratings, the grating formation time scales as the square of the grating spacing. Thus, density gratings are completely unsuitable for microwave applications, as typical formation times are on the order of days. However, the time it takes for a 10 μ particle to rotate through π radians is on the order of seconds, so that nonlinear optics using static orientational gratings in shaped microparticle suspensions are quite feasible at long wavelengths. Note, that the slow medium response times preclude the possibility of carrying out any frequency-mixing processes such as harmonic, frequency-difference or frequency-sum generation.

As a natural follow on of this research we are presently exploring a new class of artifical dielectrics, namely optomechanical media [14], [15]. These active media consist of a three-dimensional array of electrically small, anisotropic particles. These particles are supported by some mechanical means, and are free to either roll or reorient via the action of electrostrictive forces and torques generated by polarized radiation. These electrostrictive torques are similar to those discussed in this paper as they rotate the particles into a preferred direction set by the net polarization vector of the incident radiation. Rotation of the particles gives rise to orientation index gratings that can be used for active optical processes.

In conclusion, we note that in the past ten years optical phase conjugation, at visible and infrared wavelengths, has stirred intense interest in the scientific and engineering communities. This attention arises from the fundamental scientific significance as well as the vast number of important applications for this process. Until these studies were initiated very little had been achieved with regards to generating phase conjugate radiation at microwave and millimeter wavelengths. This statement is underscored by the enormous investment in communication and other equipment that modern nations have in this region of the spectrum. Obvious applications to radar, navigation and microwave communications as well as the salient scientific value of materials research and fundamental nonlinear optics justifies detailed research into achieving microwave phase conjugation. We hope that this work demonstrates the feasibility of working in this area and will stimulate research towards phase conjugation at these long wavelengths in other nonlinear media.

Acknowledgment

UCLA acknowledges partial support by the Air Force Office of Scientific Research.

References

[1] Y. R. Shen, *The Principles of Nonlinear Optics*. New York: Wiley, 1984.
[2] E. G. Hanson, Y. R. Shen, and G. Wong, *Phys. Rev.* vol. 14, p. 1281, 1986.
[3] R. W. Hellwarth, Prog. *Quantum Electron.*, vol. 5, no. 1, 1977.
[4] R. Pizzoferrato, D. Rogovin, and J. Scholl, *Opt. Lett.*, vol. 16, p. 297, 1991.
[5] R. Pizzoferrato, M. Marinelli, U. Zammit, F. Scudieri, S. Martellucci, and R. Romagnoli, *Opt. Lett.*, vol. 68, p. 231, 1988.
[6] B. Bobbs, R. Shih, H. R. Fetterman, and W. W. Ho, *App. Phys. Lett.*, vol. 52, no. 4, 1988.
[7] R. McGraw, D. Rogovin, W. Ho, B. Bobbs, R. Shih and H. Fetterman, *Phys. Rev. Lett.*, vol. 61, p. 943, 1988.
[8] R. Shih, H. Fetterman, W. Ho, R. McGraw, D. Rogovin, and B. Bobbs, *Phys. Rev. Lett.*, vol. 65, p. 579, 1990.
[9] —, *SPIE*, vol. 1220, p. 46, *Nonlinear Optics*, 1990.
[10] A. Ashkin, J. M. Dziedzic, and P. W. Smith, *Optics Lett.*, vol. 7, p. 276, 1982.
[11] P. W. Smith, A. Ashkin, J. E. Bjorkholm, and D. J. Eilenberger, *Optics Lett.*, vol. 10, p. 276, 1984.
[12] P. W. Smith, A. Ashkin, and W. J. Tomlinson, *Optics Lett.*, vol. 6, p. 276, 1981.
[13] D. Rogovin, *Phys. Rev.*, A32, p. 2837, 1985.
[14] D. Rogovin and T. P. Shen, "Active opto-mechanical media for nonlinear microwave processes," *IEEE Microwave Guided Wave Lett.*, vol. 1, p. 388, 1991.
[15] D. Rogovin and T. P. Shen, "Orientational optomechanical media for microwave applications," *J. Applied Physics*, vol. 71, p. 5281, 1991, as a Communication.

D. Rogovin received the Ph.D. from the University of Pennsylvania in 1970 in theoretical physics, specializing in superconductivity and Josephson tunneling.

He went from there to Massachussetts Institute of Technology and following that to the Optical Science Center at the University of Arizona where he did fundamental studies in quantum and nonlinear optics, laser physics and superconductivity. He then joined Science Applications, Inc, where he continued this work. Following this, he joined Rockwell Science Center as a Member of the Technical Staff and for the last five years, as manager of the Mathematical Physics Group. Dr. Rogovin has published over 100 papers in physics and engineering literature.

R. L. McGraw received the B.S. degree in 1972 from Drexel University, and the M.S. and Ph.D. degrees from the University of Chicago in 1974 and 1979, respectively.

He is presently a member of Technical Staff, Rockwell International Science Center. At the Science Center since 1985, Dr. McGraw is currently engaged in studies of nucleation and nonlinear optics and is Program Manager for several programs in these areas. From 1980 to 1985 he held a scientific staff position in the Environmental Chemistry Division, Brookhaven National Laboratory. From 1977 to 1980 he was a postdoctoral research associate in the Chemistry Department at UCLA.

W. W. Ho is a member of the technical staff in the Applied Spectroscopy Department at Rockwell International Science Center. He joined the Science Center upon obtaining his Ph.D. from the Physics Departmrnt of Columbia University in 1967. Dr. Ho's current research interests include electromagnetic properties of matter and novel optical and microwave device concept development which utilizes various nonlinear properties of advanced materials.

R. Shih, photograph and biography not available at the time of publication.

H. R. Fetterman, photograph and biography not available at the time of publication.

B. Bobbs, photograph and biography not available at the time of publication.